Controlled Strain on a Double-Templated Textured Polymer Film: a New Approach to Patterned Surfaces with Bravais Lattices and Chains

Mingwei Zhu, Yumei Li, Tao Meng, Peng Zhan, Jie Sun, Jun Wu, Zhenlin Wang,* Shining Zhu, and Naiben Ming

National Laboratory of Solid State Microstructures, Nanjing University, Nanjing 210093 P. R. China

Received March 6, 2006. In Final Form: May 25, 2006

A double template-assisted fabrication method for making surface patterns with tunable lattice geometries on a polymer surface is reported. This technique is based on a locally nonuniform strain produced in a double-templated polymer film that has a strong modulation in thickness. It can produce all 2D primitive Bravais lattices as well as chains on the surface of a polymer. The lattice parameters are controllable with nanoprecision by varying the direction and amount of the applied strain.

Introduction

Regular two-dimensional (2D) nano- and microstructures have been extensively studied for their wide range of applications in modern science and technology.[1−4] For example, solely modification in surface topography can yield a remarkable tailoring of hydrophobicity properties of a polymer surface,[5−7] modification of protein adsorption, cell adhesion on polymer substrates,[8−10] etc.

Up to now, various techniques have been reported for surface topography creation/modification. For example, a reaction−diffusion methodology has been developed by Grzybowski and co-workers that allows for the creation of complex surface topologies or symmetries[11−13] and a method of microscopic surface patterning by rubbing induced dewetting without the use of lithography has been reported by Zhang et al.[14] Among surface topography fabrication methods,[1−4] physical contact approaches,[15−21] including molding and printing techniques, have gained much interest in the production of nanopatterns for their simplicity, high patterning efficiency, and low cost. However, the contact methods involve the use of a mold, whose fabrication is expensive and time-consuming as it usually relies on photon,[22,23] particle,[24,25] or scanning probe[26−29] based lithography techniques and thus need complex facilities and techniques.

Another rapid but cheap way to build microstructures with periodicities from micrometers to submicrometers is the self-organization approach.[30−32] Self-assembly of monodisperse microspheres forms highly ordered 2D colloidal crystals that can be used as masks for nanosphere lithography[33−36] and as templates[37−39] to generate new functional nanostructured surfaces. Unfortunately, the surface patterns that can be generated via colloidal crystal templating are rather limited, due to its inefficiency in the control of lattice symmetry and spatial parameters.

Recently, a combination of the above methods has been proposed, as it provides a feasible route for fabrication of novel structures and to further lower the cost but still satisfy requirements for wide applications of such nanostructures. For example, controllable deformation has been introduced into the self-assembly method to control the shape of nanospheres confined in a film and to fabricate ordered arrays of nonspherical

* Corresponding author. E-mail: zlwang@nju.edu.cn.

(1) Xia, Y.; Rogers, J. A.; Paul, K. E.; Whitesides, G. M. *Chem. Rev.* **1999**, *99*, 1823.
(2) Geissler, M.; Xia, Y. *Adv. Mater.* **2004**, *16*, 1249.
(3) Wouters, D.; Schubert, U. S. *Angew. Chem., Int. Ed.* **2004**, *43*, 2480.
(4) Gates, B. D.; Xu, Q.; Stewart, M.; Ryan, D.; Willson, C. G.; Whitesides, G. M. *Chem. Rev.* **2005**, *105*, 1171.
(5) Gu, Z.-Z.; Uetsuka, H.; Takahashi, K.; Nakajima, R.; Onishi, H.; Fujishima, A.; Sato, O. *Angew. Chem. Int. Ed.* **2003**, *42*, 894.
(6) Shiu, J.-Y.; Kuo, C.-W.; Chen, P.; Mou, C.-Y. *Chem. Mater.* **2004**, *16*, 561.
(7) Lu, X.; Zhang, J.; Zhang, C.; Han, Y. *Macromol. Rapid Commun.* **2005**, *26*, 637.
(8) Curtis, A.; Wilkinson, C. *Biomaterials* **1997**, *18*, 1573.
(9) Ostuni, E.; Yan, L.; Whitesides, G. M. *Colloids Surf. B: Biointerfaces* **1999**, *15*, 3.
(10) Denis, F. A.; Hanarp, P.; Sutherland, D. S.; Gold, J.; Mustin, C.; Rouxhet, P. G.; Dufrêne, Y. F. *Langmuir* **2002**, *18*, 819.
(11) Campbell, C. J.; Klajn, R.; Fialkowski, M.; Grzybowski, B. A *Langmuir* **2005**, *21*, 418.
(12) Campbell, C. J.; Baker, E.; Fialkowski, M.; Bitner, A.; Smoukov, S. K.; Grzybowski, B. A. *J. Appl. Phys.* **2005**, *97*, 126102.
(13) Campbell, C. J.; Baker, E.; Fialkowski, M. B.; Grzybowski, A. *Appl. Phys. Lett.* **2004**, *85*, 1871.
(14) Zhang, X.; Xie, F.; Tsui, Ophelia, K. C. *Polymer* **2005**, *46*, 8416.
(15) Schift, H.; Heyderman, L. J.; Auf der Maur, M.; Gobrecht, J. *Nanotechnology* **2001**, *12*, 173.
(16) Geissler, M.; McLellan, J. M.; Chen, J.; Xia, Y. *Angew. Chem., Int. Ed.* **2005**, *44*, 3596.
(17) Yang, S. M.; Ozin, G. A. *Chem. Commun.* **2000**, 2507.
(18) Xia, Y.; Whitesides, G. M. *Angew. Chem., Int. Ed. Engl.* **1998**, *37*, 550.
(19) Chou, S. Y.; Krauss, P. R.; Renstrom, P. J. *Appl. Phys. Lett.* **1995**, *67*, 3114.
(20) Guo, L. J. *J. Phys. D: Appl. Phys.* **2004**, *37*, R123.
(21) Xia, Y.; Whitesides, G. M. *Langmuir* **1997**, *13*, 2059.
(22) Switkes, M.; Kunz, R. R.; Rothschild, M.; Sinta, R. F.; Yeung, M.; Baek, S.-Y. *J. Vac. Sci. Technol. B* **2003**, *21*, 2794.
(23) Switkes, M.; Rothschild, M. *J. Vac. Sci. Technol. B* **2001**, *19*, 2353.
(24) Bedson, T. R.; Palmer, R. E.; Jenkins, T. E.; Hayton, D. J.; Wilcoxon, J. P. *Appl. Phys. Lett.* **2001**, *78*, 1921.
(25) Karmous, A.; Cuenat, A.; Ronda, A.; Berbezier, I.; Atha, S.; Hull, R. *Appl. Phys. Lett.* **2004**, *85*, 6401.
(26) Hoogenboom, J. P.; Vossen, D. L. J.; Faivre-Moskalenko, C.; Dogterom, M.; van Blaaderen, A. *Appl. Phys. Lett.* **2002**, *80*, 4828.
(27) García-Santamaría, F.; Miyazaki, H. T.; Urquía, A.; Ibisate, M.; Belmonte, M.; Shinya, N.; Meseguer, F.; López, C. *Adv. Mater.* **2002**, *14*, 1144.
(28) Junno, T.; Deppert, K.; Montelius, L.; Samuelson, L. *Appl. Phys. Lett.* **1995**, *66*, 3627.
(29) Ginger, D. S.; Zhang, H.; Mirkin, C. A. *Angew. Chem., Int. Ed.* **2004**, *43*, 30.
(30) Jiang, P.; Bertone, J. F.; Hwang, K. S.; Colvin, V. L. *Chem. Mater.* **1999**, *11*, 2132.
(31) Wong, S.; Kitaev, V.; Ozin, G. A. *J. Am. Chem. Soc.* **2003**, *125*, 15589.
(32) Kim, E.; Xia, Y.; Whitesides, G. M. *J. Am. Chem. Soc.* **1996**, *118*, 5722.
(33) Zhang, G.; Wang, D.; Möhwald, H. *Nano. Lett.* **2005**, *5*, 143.
(34) Kosiorek, A.; Kandulski, W.; Glaczynska, H.; Giersig, M. *Small* **2005**, *1*, 439.
(35) Choi, D.-G.; Yu, H. K.; Jang, S. G.; Yang, S.-M. *J. Am. Chem. Soc.* **2004**, *126*, 7019.
(36) Hulteen, J. C.; Van Duyne, R. P. *J. Vac. Sci. Technol. A* **1995**, *13*, 1553.
(37) Jiang, P.; Bertone, J. F.; Colvin, V. L. *Science* **2001**, *291*, 453.
(38) Wu, M.-H.; Whitesides, G. M. *Appl. Phys. Lett.* **2001**, *78*, 2273.
(39) Piglmayer, K.; Denk, R.; Bäuerle, D. *Appl. Phys. Lett.* **2002**, *80*, 4693.

10.1021/la060617f CCC: $33.50
Published on Web 07/20/2006

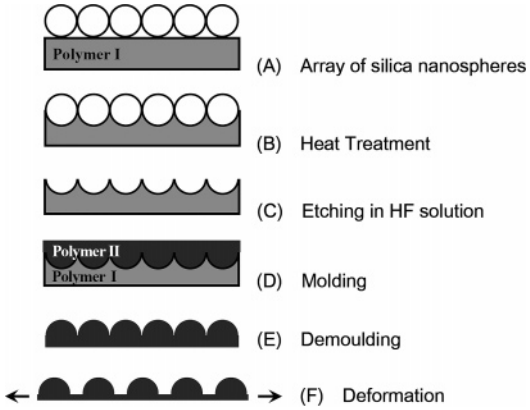

Figure 1. Schematic for fabricating ordered nanopatterns on a polymer surface, using an inhomogeneous deformation approach.

nanospheres.[40,41] Very recently, polymer deformation has been integrated into soft lithography to tune the separations between particles anchored on a polymer film surface.[42] However, the development of methods for fabricating a nanostructured surface pattern with a controllable lattice symmetry, high efficiency, as well as low cost remains open.

It is known that many glassy polymers have a yielding behavior below their glass-transition temperature (T_g) with the following features.[43] For low stresses, the materials have a time-independent linear elastic behavior and with full recovery of strain on removal of stress. For stresses above a certain level, called yield stress, the polymer yields. During this process, the strain increases without further increase in the stress. After yielding, the polymer retains a permanent deformation on removal of the stress. Thus for a patterned polymer foil with a strong modulation in thickness, it is possible to make selective deformations in the polymer because the area with bumps can remain below the yield stress and thus preserve the shape. Such an inhomogeneous deformation can lead to a variation of the unit cell of a 2D topographically patterned surface of organic foils.

Herein we present a new avenue to fabrication of polymer films with a variety of two-dimensionally patterned surfaces, of which both the lattice geometry and the lattice constants are controllable. Our technique is based on a locally nonuniform strain produced in a double-templated polymer film that has a sharp modulation in thickness. We show that all 2D primitive lattices can be created on such a polymer film surface through controlled deformations. The present method can provide a simple, rapid, and inexpensive approach for fabricating ordered surface patterns. We also show that the method could be further extended to control the distribution of nanoparticles on a polymer surface.

Experimental Section

Outline of the Experiment. The sharp variations in thickness as well as the periodicity in our polymer films are fabricated through a double-templated imprint procedure. Figure 1 shows the experimental outlines. First, a negative polymer nanomold is fabricated during the imprint process (steps from A to C). Here, a hexagonally close-packed monolayer of silica beads is prepared on a polymer film (referred to as polymer I). Then the organic substrate is heated above its glass transition temperature, and hence, the silica beads are imprinted partially into the polymer film surface under the force of gravity (hot embossing imprint).

After cooling followed by immersion in an HF solution for removal of silica beads, a uniform and hemispherical cavities array is created on the polymer I surface. Using this modulated polymer further as a nanomold, another polymer (referred to as polymer II) with a microstructured surface can be replicated via a second hot embossing imprint process (steps D and E), of which a sharp and periodic variation in thickness is introduced. By mechanically pressing polymer I mold against polymer II foil, while heating polymer II slightly above its T_g, a replica with segmented hemispherical particles array is created on polymer II surface. Note that, for this imprint, polymer II is required to have a lower T_g as compared to polymer I. Finally, the sharply modulated organic membrane is drawn to undergo controllable deformations to obtain polymer films with different surface patterns.

Fabrication of Polycarbonate Micromold. As examples of demonstration, we choose polycarbonate (PC) as polymer I and polyethylene (PE) as polymer II. PC has a relatively high glass transition temperature (T_g = 145 °C), low elasticity, and excellent deformation resistivity. These properties enable PC polymer to be used as a rigid mold for patterning other polymers having a lower T_g. PE has a unique feature of large stain in yield behavior as well as a lower T_g (T_g = 105 °C) and thus can be manipulated with controllable deformations. A PC substrate (0.6 mm in thickness) was immersed in an aqueous solution of sodium dodecyl sulfate (1.0 wt %) for 5 min to make its surface hydrophilic. Monodisperse silica spheres of 1.59 μm in diameter (size dispersion of 3%, purchased from Duke Company) were assembled on the PC membrane to prepare a hexagonal close-packed array of silica spheres, using the published method.[44] Then, the sample was placed horizontally in an oven (160 °C) for about 0.5 h to let the spheres semi-embedded into the surface of the PC substrate. After cooling to ambient temperature, the sample was immersed in an HF solution (45%) for 10 min to dissolve the silica beads. The resulted PC replica had a 2D hexagonal array of hemispherical cavities.

Patterning Polyethylene Membranes by Molding. A PE film of about 10 μm in thickness was placed on a flat glass substrate. Then the PC mold with the patterned side facing the PE template was brought into contact with the PE membrane. A piece of filter paper and another piece of glass plate were placed on sequentially. The whole structure was clipped and kept in oven at 120 °C for 20 min to ensure an adequate pattern transfer. The filter paper served as a buffer layer for an even distribution of the pressure. After cooling to ambient temperature, the PE film was peeled off from the PC mold, leaving a 2D hexagonal close-packed array of hemispherical bumps on its surface. Note that the PC mold can be used repeatedly without any deformation or contamination due to the "self-cleaning" characteristic of hot embossing.[1]

Formation of Patterned Surfaces by Inhomogeneous Deformations. The created PE membrane was then put under drawings. For a controllable drawing, homemade equipment was used that consisted of a framework with guide rails, a screw micrometer (a minimum scale of 0.01 mm) fixed on one end of the framework, and a slider that can be drawn by the screw micrometer to slip on the guide rails. Before drawing, the patterned PE film was adjusted to the needed lattice orientation in relative to the drawing direction. Then the screw micrometer knob was rotated slowly to let the film extend until a designed draw ratio is achieved. Holding on the load, the film was annealed in an oven at 80 °C for 5 min to eliminate the residual inner stress so as to avoid shrinkage after removal of the load. The above process was repeated when multistep drawings are needed.

Morphology Characterization. Characterization of the samples was conducted using a scanning electron microscope (XL30, Philips) with primary electron energy of 20 kV; a 10 nm thick layer of gold was sputtered (Model 682, Gatan) onto samples to facilitate the imaging. The patterned PE films were snipped to reveal their cross-sections.

(40) Mohraz, A.; Solomon, M. J. *Langmuir* **2005**, *21*, 5298.
(41) Keville, K. M.; Franses, E. I.; Caruthers, J. M. *J. Colloid Interface Sci.* **1991**, *144*, 103.
(42) Yan, X.; Yao, J.; Lu, G.; Li, X.; Zhang, J.; Han, K.; Yang, B. *J. Am. Chem. Soc.* **2005**, *127*, 7688.
(43) Bower, David I. *An Introduction to Polymer Physics*; Cambridge University Press: New York, 2002,; p 220.
(44) Chen, Z.; Zhan, P.; Wang, Z. L.; Zhang, J. H.; Zhang, W. Y.; Ming, N. B.; Chan, C. T.; Sheng, P. *Adv. Mater.* **2004**, *16*, 417.

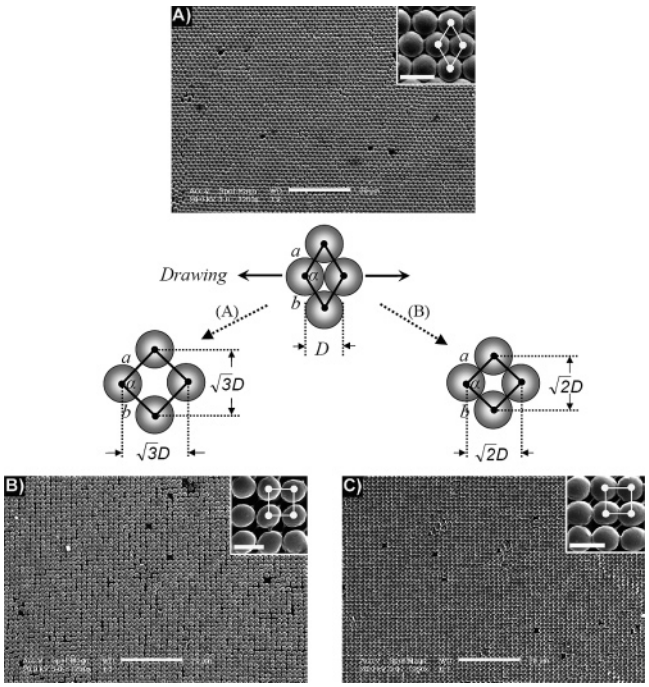

Figure 2. Schematic illustration of transformation of a modulated PE membrane with a hexagonal lattice to a square lattice via 1D and 2D deformations and the SEM images of the corresponding typical samples. (A) SEM image of the as-templated hexagonal lattice; (B and C) SEM images of the resultant square lattices after 1D and 2D deformations, respectively. Scale bars are 20 and 2 μm (insets).

Results and Discussion

Figure 2A shows the scanning electron microscopy (SEM) image of a textured PE film through the double templating process. It is seen that the fabricated PE membrane surface was decorated with a hexagonal array of segmented spheres with a highly uniform shape and periodic distribution. These well-defined hemispherical particles reflect exactly the order, symmetry, and shape of the cavities array created in the intermediate PC mold. This also shows that the partial embedment of the primary silica microbeads into the PC foil was quite uniform. Such properties stem from the advantages of the hot embossing nanoimprint technique[15] as it can transfer patterns from a mold into a thin polymer film with high uniformity, efficiency, and fidelity. Note that the created bumps on polymer II surface had a slightly smaller lattice constant (1.45 μm) as compared to the primary silica colloidal template (1.59 μm). This resulted from the shrinkages of the PC and PE mold during imprinting. Due to such a sharply modulated thickness of the PE polymer film, an inhomogeneous stress distribution is produced upon loading with the consequence of nonuniform strains. We use such a property to achieve transformations among 2D lattices with different symmetries or the same lattice type but with different lattice constants.

Basically, a 2D lattice is described with two translation vectors (a and b) and the angle (α) between them. The as-prepared PE film has a patterned surface with a hexagonal lattice (HL), i.e., $a = b$ and $\alpha = 120°$ (Figure 2A). In the following, we first show that such a HL can be transformed to a square lattice (SL) with $a = b$ and $\alpha = 90°$, through one-dimensional (1D) or 2D deformations (Figure 2, panels B and C).

The magnitude of a deformation is usually described with a draw ratio δ defined as $\{(l - l_0)\}/\{l_0\}$, where l_0 and l are the lengths of a sample before and after stretching, respectively. For a sample of which the length along the drawing direction is much smaller than that along the orthogonal direction, the stretching can be approximated as a 1D deformation because the strain perpendicular to the drawing is negligible. In the opposite cases, i.e., when the length along drawing is much larger, the deformation should be treated as a 2D one, of which the sample will undergo a simultaneous reduction in length along the perpendicular direction as well as an increase in length along the draw axis. Other situations can be considered as a mixture of the two extremities. For simplicity, only the 1D and 2D cases are discussed and exploited here. In the following, we show that the resultant lattice type can be controlled by monitoring the drawing direction, draw ratio, and the type (1D or 2D) of deformation, by choosing SL as the example.

For the use of a 1D deformation (Figure 2, process A), a modulated PE film is put under a load along the (11) direction of a HL. In this case the segmented spheres on the mesh surface will move apart along the drawing direction, while keeping their separations in the perpendicular direction. As a consequence, the angle α decreases continuously from 120°; when the draw ratio reaches a value $\delta = \sqrt{3} - 1$, a nonclose-packed SL is formed with $\alpha = 90°$ (Figure 2B).

A patterned PE film with a SL on its surface can also be formed via a 2D deformation from the original HL (Figure 2, process B). During such a 2D deformation, the adjacent spheres will be drawn apart along the drawing direction while the neighboring spheres along the axis perpendicular to the drawing direction will come closer. A SL of close-packed hemispheres is obtained on the PE membrane when the draw ratio δ reaches a value of $\sqrt{2} - 1$ (Figure 2C).

In addition to the SLs, other 2D Bravais lattices can also be formed through controllable deformations from the HL. The specific drawing processes are summarized in Table 1, with the SEM images of typical samples shown in Figure 3. The primitive units of these 2D ordered patterns are described, respectively, with $a = b$ and $\alpha \neq 90°$ or 120° for rhombus lattice, $a \neq b$ and $\alpha = 90°$ for a rectangular lattice, and $a \neq b$ and $\alpha \neq 90°$ for a parallelogrammic lattice, the most general 2D lattice. The rhombus lattice shown in Figure 3A was obtained through a 2D deformation with a draw ratio $\delta = 0.25$ along the (11) direction of the original HL; the rectangular lattice in Figure 3B was created from an intermediate SL, by an additional drawing along the (01) direction of the square lattice with a draw ratio of 0.25; the parallelogrammic lattice in Figure 3C was obtained by applying a drawing along the (01) direction of a rhombus lattice with a draw ratio of 0.5.

From the SEM images shown in Figure 3, it is seen that the PE particles connected with the supported PE film were distributed with highly uniform separations; long-range ordering was well preserved after multiple drawings. Slight distortions from hemispherical shape are visible from the insets shown in Figure 3A-C and such distortions came from small anisotropic deformations at the particle edge after stretching. A tilted view of the cross-section of the film before and after drawings was shown in Figure 3, panels D and E, respectively, with their top views presented in Figures 2A and 3C. It can be seen from Figure 3D that the substrate connecting the hemispheres was quite uniform. Here the modulation depth of the film is only about a tenth of the film thickness. The sharp contrast due to the formation of bumps on the original film was still maintained after stretching. Nevertheless, the inhomogeneous deformation in the particle shape led to a slight decrease in the modulation contrast. In Figures 2 and 3, defects (mostly voids), which were born from the primary silica template, are also observed but seem to have negligible effect on the surrounded particle distributions. These results demonstrate that it is quite feasible to prepare an organic membrane having a periodically patterned surface with any types

Table 1. Summary of the Drawing Steps for Transforming a HL to Rhombic, Rectangular, and Parallelogrammic Bravais Lattices

Drawing Step 1		Midterm Lattice Type	Drawing Step 2		Final Lattice Type
Direction	Ratio		Direction	Ratio	
←→	0.25*				rhombus
←→	$\sqrt{2}-1$*	square	↗↙	0.25	rectangle
←→	0.25*	rhombus	↗↙	0.5	parallelogram

*2D deformation; others through1D deformations.

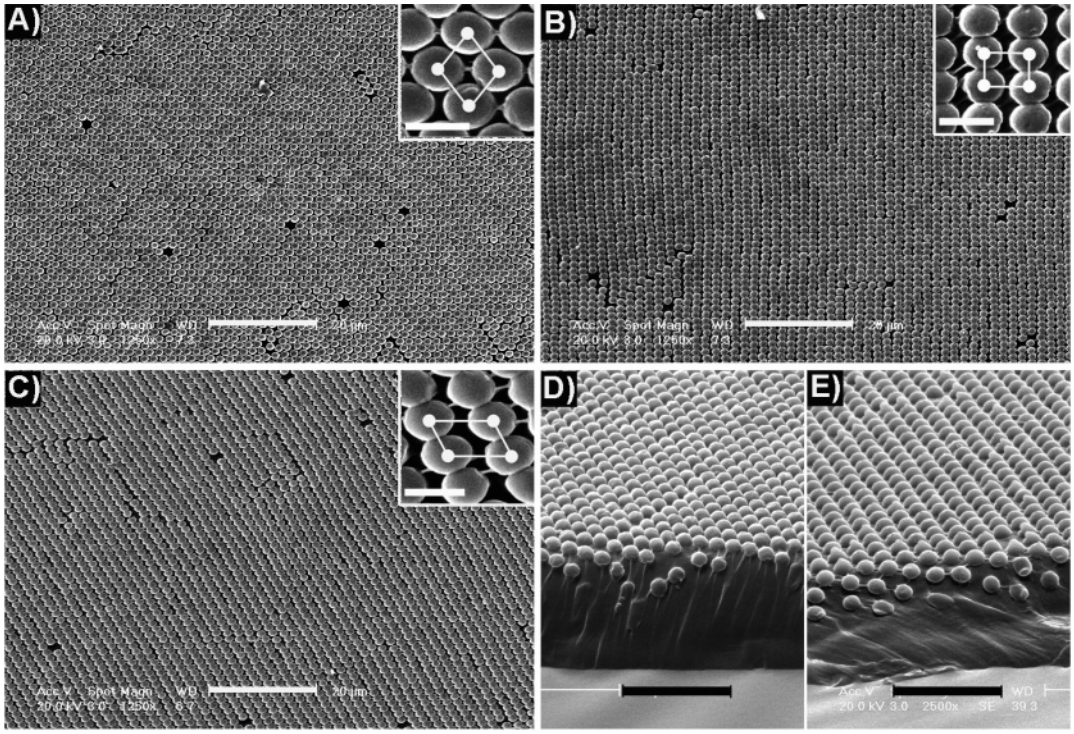

Figure 3. SEM images (top view) of a textured PE film with 2D patterns of different lattice types on its surface. (A) Rhombus; (B) rectangle; (C) parallelogram. Shown in the inset in each figure is the image at a higher magnification with the unit cell indicated. Panels D and E show the cross-sectional images of the film before and after stretching, respectively. Scale bars are 20 μm in panels A−C, 2 μm in the inset, and 10 μm in panels D and E.

of 2D lattice, using the present double-templating and transformation method.

In addition to the creation of different lattice types, the present method also allows a high-degree tuning of the lattice constants. Here the lattice constants of the above 2D lattices can be adjusted independently by two sequential deformations. For example, when the PE mesh (Figure 2A) is drawn along the (10) [or (01)] direction under a 1D deformation, the lattice parameter a along the corresponding axis will be varied, with the value of α unchanged. The lattice type will remain the same when another 1D deformation is performed at the same draw ratios, both along the two primitive vectors of the original HL. Typical experimental results are presented in Figure 4, which are fabricated by applying two separate 1D drawings along the (01) and (10) directions of a HL under identical draw ratios. We measured the lattice parameter (a) of these HLs made with differing draw ratios ($\delta_A = 0.05$, $\delta_B = 0.10$, and $\delta_C = 0.20$). The sample in Figure 4A has a lattice constant of 1.52 ± 0.04 μm; the sample in Figure 4B has a lattice constant of 1.58 ± 0.05 μm; the sample in Figure 4C has a lattice constant of 1.70 ± 0.07 μm. In these cases, the primary PE membrane with a HL has a lattice constant of 1.45 ± 0.03 μm. Thus, the induced relative increase in the lattice constant is 4.8% in Figure 4A, 9.0% in Figure 4B, and 17.2% in Figure 4C and is found to agree well with the predicted value under the corresponding draw ratio.

A large contrast in the draw ratios of two separate drawings can lead to patterned surfaces containing microbumps in a straight line with uniform interparticle separation and interchain spacing. Figure 5 shows the SEM images of the typical samples, of which their preparation was accomplished through two successive 1D deformations: the first draw was along the (12) direction of a HL to achieve a specific line spacing (s), followed by another drawing but along the line axis to control the interparticle distance (d). The line spacing and interparticle distance can be tuned from tens of nanometers to a few micrometers, by changing the relative value of the draw ratios (Figure 5). It is noted that a draw ratio

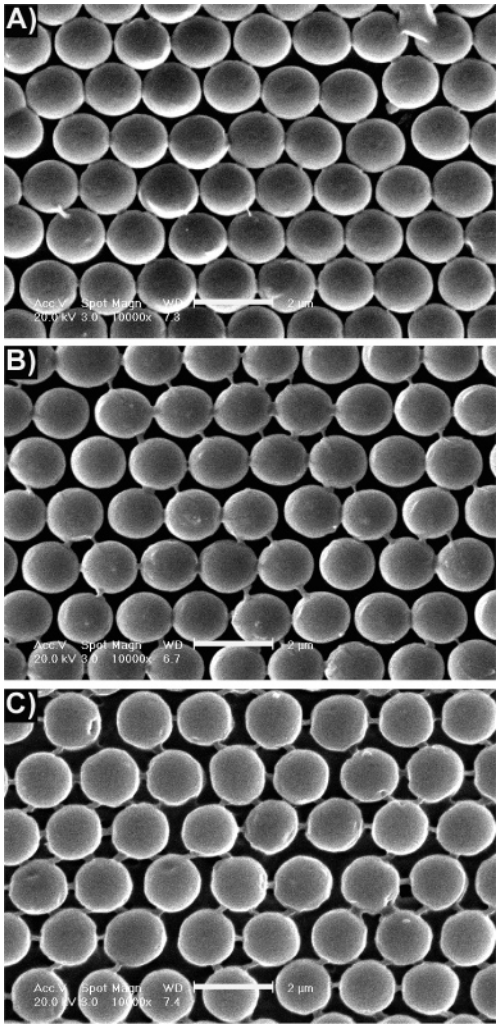

Figure 4. SEM images of PE membranes with a hexagonal array of particles. These samples are templated from the same silica template and deformed using different draw ratios: $\delta = 0.05$ (A), $\delta = 0.10$ (B), and $\delta = 0.20$ (C). Scale bar 2 μm.

larger than 5.0 is not feasible in our experiment, because the PE film begins to tear under such an excessive strain. The use of polymers with larger strain tolerance may alleviate this problem.

Many sophisticated particle manipulation techniques, including optical tweezers,[26] microrobot,[27] and atomic force microscopy,[28,29] have been demonstrated and can place a nanoparticle precisely at a desired position on a substrate. Besides the fabrication of polymer films with a variety of patterned surfaces, we show that the present method can also be extended to manipulate spatial distribution of nanoparticles on a 2D plane. To achieve this, nanoparticles are required first to be introduced, via a proper method, into the cavities formed in the PC mold. Then the molding and demolding processes (Figure 1, steps D and E) can transfer these nanoparticles from the bottom of the voids onto the top of each PE hemisphere. Through the drawing processes discussed above, the nanoparticles will change their relative positions as their carriers, i.e., the hemispheres, are moved on a 2D plane in a collective way.

We use silica nanospheres as an example to demonstrate such a manipulation process. Here the introduction of a silica nanosphere into a cavity on the PC mold is achieved through partially etching the primary silica beads in a vapor of HF by controlling the etching duration. The created PC mold, now containing a silica nanoparticle in each void, is used to pattern a PE film (Figure 1D). After this step, the inorganic nanoparticles

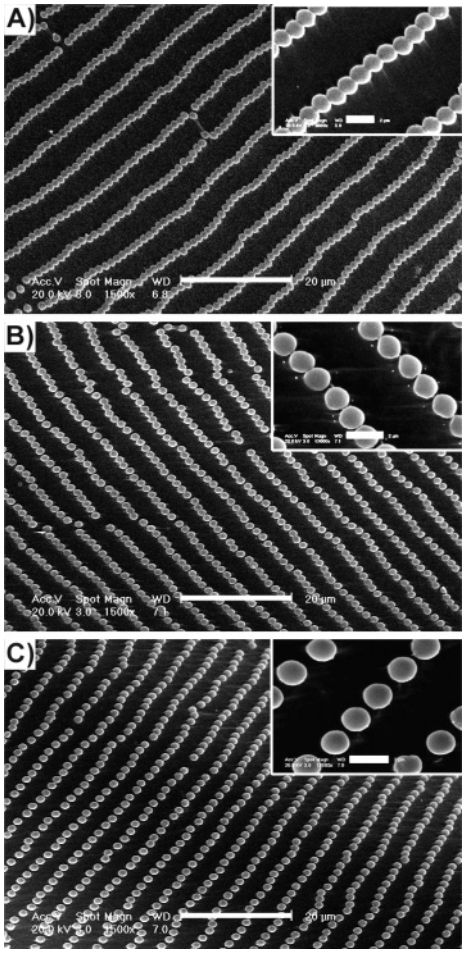

Figure 5. SEM images of PE surfaces patterned with particle chains templated from a monolayer of silica spheres ($D = 1.59$ μm), using different set of 1D drawings. The two separate draw ratios are, respectively, (3.2, 0.0) (A), (2.2, 0.3) (B), and (2.0, 0.6) (C). These samples have different chain spacings (s) and center-to-center particle distances (*d*). (A) $s = 5.98$ μm and $d = 1.44$ μm; (B) $s = 4.54$ μm and $d = 1.87$ μm; (C) $s = 4.21$ μm and $d = 2.13$ μm. Scale bars are 20 μm in panels A−C and 2 μm in the insets.

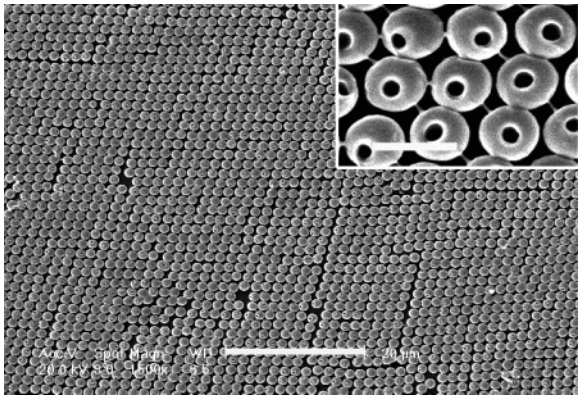

Figure 6. SEM image of a textured PE film after the silica nanoparticle on the top of each segmented sphere was etched out. Due to the dissolution of the silica particles, a nanocavity was formed on the surface of each PE sphere. The inset shows a higher magnification of the sample. Scale bars are 20 and 2 μm (inset).

are embedded on the salience of the templated PE mesh that is put under a transformation to a parallelogrammic lattice. To see that each hemisphere surface is embedded with a silica nanosphere, the deformed membrane is immersed in a HF solution. The SEM analysis (Figure 6) shows that a nanocavity on the top

of each PE hemisphere is formed because the silica nanospheres are etched away, thus leaving a nanocavity on the surface of each PE particle. The present manipulation method has the advantages of simplicity as well as high-throughput. We expect that it could be extendable to 2D manipulation of metal or semiconductor nanoparticles.

Conclusion

In summary, we have presented a new, rapid, and inexpensive strategy for fabricating polymer membranes with 2D patterns based on inhomogeneous deformation of a double templated textured polymer film. The preparation of all of the primitive 2D Bravais lattices and particle chains is demonstrated with precisely tunable structure parameters. The present method can also be extended to a collective manipulation of inorganic nanoparticles within a 2D plane. The prepared patterned polymer film can further be used as templates to prepare other patterns,[45−47] as a microlens system to focus light and thereby generate small structures,[38,39] or as substrates to tailor the surface hydrophobicity.[5−7] Other potential applications could be found in organic-based optoelectronic devices by incorporation of active compounds[48] and in plasmon-based devices with the possible decoration of metal nanoparticles where particle−particle interaction is important.[49,50]

Acknowledgment. This work is supported by a grant for the State Key Program for Basic Research of China and by NSFC under Grant Nos. 10425415 and 90501006. Z.L.W. is grateful for the Distinguished Youth Foundation of NSFC.

LA060617F

(45) Yin, Y.; Xia, Y. *Adv. Mater.* **2002**, *14*, 605.

(46) Ye, Y.-H.; Badilescu, S.; Truong, Vo-Van; Rochon, P.; Natansohn, A. *Appl. Phys. Lett.* **2001**, *79*, 872.

(47) Yin, Y.; Xia, Y. *J. Am. Chem. Soc.* **2003**, *125*, 2048.

(48) Barbarella, G.; Favaretto, L.; Sotgiu, G.; Zambianchi, M.; Bongini, A.; Arbizzani, C.; Mastragostino, M.; Anni, M.; Gigli, G.; Cingolani, R. *J. Am. Chem. Soc.* **2000**, *122*, 11971.

(49) Hicks, E. M.; Zou, S.; Schatz, G. C.; Spears, K. G.; Van Duyne, R. P.; Gunnarsson, L.; Rindzevicius, T.; Kasemo, B.; Käll, M. *Nano. Lett.* **2005**, *5*, 1065.

(50) Maier, S. A.; Kik, P. G.; Atwater, H. A.; Meltzer, S.; Harel, E.; Koel, B. E.; Requicha, A. A. G. *Nat. Mater.* **2003**, *2*, 229.